

Radiative Effects of Stratospheric Seasonal Cycles in the Tropical Upper Troposphere and Lower Stratosphere

DANIEL M. GILFORD AND SUSAN SOLOMON

Department of Earth, Atmospheric and Planetary Sciences, Massachusetts Institute of Technology, Cambridge, Massachusetts

(Manuscript received 30 August 2016, in final form 20 December 2016)


ABSTRACT

Water vapor and ozone are powerful radiative constituents in the tropical lower stratosphere, impacting the local heating budget and nonlocally forcing the troposphere below. Their near-tropopause seasonal cycle structures imply associated “radiative seasonal cycles” in heating rates that could affect the amplitude and phase of the local temperature seasonal cycle. Overlying stratospheric seasonal cycles of water vapor and ozone could also play a role in the lower stratosphere and upper troposphere heat budgets through nonlocal propagation of radiation. Previous studies suggest that the tropical lower stratospheric ozone seasonal cycle radiatively amplifies the local temperature seasonal cycle by up to 35%, while water vapor is thought to have a damping effect an order of magnitude smaller. This study uses *Aura* Microwave Limb Sounder observations and an offline radiative transfer model to examine ozone, water vapor, and temperature seasonal cycles and their radiative linkages in the lower stratosphere and upper troposphere. Radiative sensitivities to ozone and water vapor vertical structures are explicitly calculated, which has not been previously done in a seasonal cycle context. Results show that the water vapor radiative seasonal cycle in the lower stratosphere is not sensitive to the overlying water vapor structure. In contrast, about one-third of ozone’s radiative seasonal cycle amplitude at 85 hPa is associated with longwave emission above 85 hPa. Ozone’s radiative effects are not spatially homogenous: for example, the Northern Hemisphere tropics have a seasonal cycle of radiative temperature adjustments with an amplitude 0.8 K larger than the Southern Hemisphere tropics.

1. Introduction

Hemispheric asymmetries in stratospheric wave driving suggest a seasonal cycle in tropical lower-stratospheric upwelling (e.g., Yulaeva et al. 1994; Rosenlof 1995; Randel et al. 2002a,b; Ueyama and Wallace 2010; Fueglistaler et al. 2011). Whereas dynamical forcing in each hemisphere commonly maximizes in its respective winter season, Northern Hemisphere wave driving is large compared with Southern Hemisphere wave driving. Consequently, there is stronger tropical lower-stratospheric upwelling in boreal

winter than in boreal summer. Corresponding to this seasonal cycle in upwelling are seasonal cycles in temperature, water vapor, and ozone above the tropical tropopause [among other tracerlike chemical constituents such as carbon monoxide; Schoeberl et al. (2006, 2008); Folkins et al. (2006); Abalos et al. (2012, 2013)], each with distinct spatial patterns of variability (e.g., Fueglistaler et al. 2009a; Ploeger et al. 2011). A portion of the tropical lower-stratospheric temperature seasonal cycle is likely related to the dynamically driven ozone seasonal cycle through radiative amplification (Chae and Sherwood 2007; Fueglistaler et al. 2011). Water vapor and ozone are strong radiatively active constituents in the tropical lower stratosphere, having both local radiative impacts on temperature and long-term implications for radiative forcing of climate change (Forster et al. 1997; Forster and Shine 1999; Stuber et al. 2001; Gettelman et al. 2004; Randel et al. 2006; Solomon et al. 2010; Maycock et al. 2011, 2014; Dessler et al. 2013; Gilford et al. 2016; Wang et al. 2016). In this study we investigate the radiative effects of water vapor and ozone seasonal cycles in the tropical lower stratosphere in detail. In particular, we explore radiative sensitivities to

 Denotes content that is immediately available upon publication as open access.

 Supplemental information related to this paper is available at the Journals Online website: <http://dx.doi.org/10.1175/JCLI-D-16-0633.s1>.

Corresponding author e-mail: Daniel M. Gilford, dgilford@mit.edu

DOI: 10.1175/JCLI-D-16-0633.1

© 2017 American Meteorological Society. For information regarding reuse of this content and general copyright information, consult the [AMS Copyright Policy](#) (www.ametsoc.org/PUBSReuseLicenses).

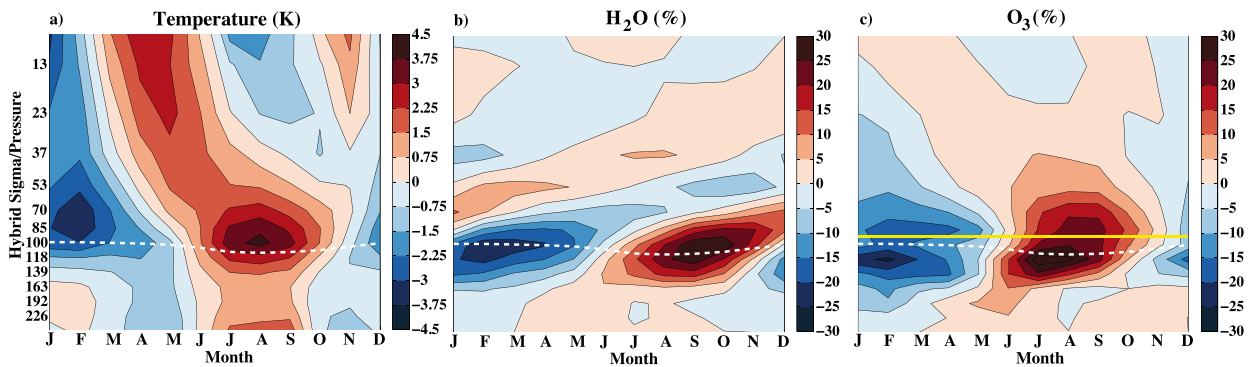


FIG. 1. Observed *Aura* MLS seasonal cycles of (a) temperature, (b) water vapor, and (c) ozone, averaged between 20°S and 20°N on PORT's grid. Contour intervals are 0.75 K in (a) and 5% in (b), (c). The white dashed curve denotes the PORT climatological tropopause averaged between 20°S and 20°N. The solid yellow line in (c) illustrates the 85-hPa pressure level used in a radiative sensitivity experiment (see text).

the overlying vertical structures of these seasonal cycles along with their latitudinal variability.

Tropical lower-stratospheric water vapor displays a consistent seasonal cycle known as the “tropical tape recorder” (Mote et al. 1996). Water vapor anomalies are created when air parcels are freeze dried as they pass upward through the cold tropopause region (e.g., Hartmann et al. 2001; Liu et al. 2007; Schoeberl and Dessler 2011). As the parcels propagate into the warmer stratosphere, water vapor anomalies are preserved, creating a “tape recorder” effect (see Fig. 1b). At any given point in a year, the consistent tape recorder spatial structure results in seasonal anomalies at higher stratospheric levels (above about 20 km) that overlie opposite-signed seasonal anomalies maximizing at lower levels near the tropopause. Mixing with older stratospheric air, increases in stratospheric water vapor from methane oxidation, and vertical diffusion jointly lead to reductions in tape recorder anomalies at middle-stratospheric altitudes (Mote et al. 1996, 1998). However, memory of tropopause temperatures in the overlying water vapor structure may still be observed up to at least 30 hPa in the tropics (see Fig. 1b).

The seasonal cycle of tropical lower-stratospheric ozone is driven primarily by local vertical advection near the tropopause (Randel et al. 2007; Schoeberl et al. 2008; Abalos et al. 2012). Unlike water vapor, ozone seasonal anomalies decay rapidly as they propagate away from their near-tropopause source because ozone's chemical lifetime becomes shorter than the transport time scale at increasing heights (e.g., Brasseur and Solomon 1986). This results in a seasonal signal in tropical lower-stratospheric ozone that is shallower than the water vapor tape recorder (see Fig. 1c). Horizontal in-mixing from the extratropics during each hemisphere's respective summer also contributes to ozone's tropical seasonal cycle, amplifying it and contributing to hemispheric asymmetries (Konopka et al. 2010; Ploeger

et al. 2011, 2012; Stolarski et al. 2014; and discussed further in sections 2 and 3). The tropical ozone seasonal cycle transitions from an annual to a semiannual cycle between about 55 and 30 hPa. The tropical semiannual oscillation in temperature (SAO; e.g., Reid 1994; Reed 1962) observed at higher-stratospheric levels (~ 30 hPa and above) is related to the semiannual signal in ozone (Hirota 1980; Maeda 1987; Perliski et al. 1989; Gebhardt et al. 2014) through chemical and radiative coupling, with a much smaller effect on water vapor (Mote et al. 1998).

Previous studies have shown that the local water vapor seasonal cycle is not very radiatively important for local lower-stratospheric temperatures, whereas local ozone changes strongly influence the seasonal cycle in tropical lower-stratospheric radiative heating (Folkins et al. 2006) and may radiatively amplify the lower-stratospheric temperature seasonal cycle by 20%–35% (Chae and Sherwood 2007; Fueglistaler et al. 2011). While some studies have examined long-term vertical radiative coupling between ozone and temperature using decadal trends (Forster et al. 2007; Grise et al. 2009), nonlocal radiative impacts associated with the overlying constituent seasonal cycles have not been previously studied. If the vertical structures do have notable nonlocal radiative effects, then accurate representation of constituent seasonal cycles with altitude would be important for evaluation of diabatic heat budgets (Fueglistaler et al. 2009b; Wright and Fueglistaler 2013). It is important to understand the radiative dependencies of near-tropopause temperatures because several processes, such as the amount of water vapor entering the stratosphere (Mote et al. 1996; Randel 2010; Randel et al. 2006; Fueglistaler et al. 2005; Fueglistaler and Haynes 2005; Schoeberl and Dessler 2011; Dessler et al. 2016) and the intensity of tropical cyclones (e.g., Bister and Emanuel 1998; Emanuel et al. 2013), are sensitive to near-tropopause temperatures.

The primary goals of this study are as follows: 1) quantify and compare the radiative impacts of observed stratospheric water vapor and ozone seasonal cycles in the tropical lower stratosphere and upper troposphere; 2) investigate the sensitivity of radiative responses to the overlying vertical structures of water vapor and ozone seasonal cycles, in order to identify local and nonlocal radiative influences; 3) separate longwave and shortwave radiative effects to determine their individual contributions to the results; and 4) elucidate the latitudinal variability of the results. The paper is organized as follows: [section 2](#) describes the satellite observations of water vapor and ozone seasonal cycles along with the broadband radiative transfer model used to calculate their radiative impacts; radiative calculations, sensitivity test results, and the latitudinal variability of results are discussed in [section 3](#); and conclusions are summarized in [section 4](#).

2. Data and methods

a. Observations

To study the radiative impacts of constituent seasonal cycles, this study uses observations of water vapor, ozone, and temperature from the *Aura* Microwave Limb Sounder (MLS) level-2 version 3.3 dataset ([Livesey et al. 2011](#); [NASA 2014](#)). MLS observations from 2005 to 2013 are quality controlled according to NASA's quality field recommendations and gridded onto a $5^\circ \times 5^\circ$ horizontal grid. MLS data stretches from the upper troposphere to the stratosphere, with 31 recommended useful vertical levels for water vapor observations (316 to 1 hPa) and 29 recommended useful vertical levels for ozone and temperature observations (261 to 1 hPa). *Aura* MLS measurements of water vapor and ozone compare well with multi-instrument means in the tropical lower stratosphere (see [Tegtmeier et al. 2013](#); [Hegglin et al. 2013](#)), and they can resolve horizontal structures that were not available with previous satellite instruments [such as the Halogen Occultation Experiment (HALOE); see [Gilford et al. \(2016\)](#)]. The ~ 300 -km native horizontal resolution in the tropical tropopause region is fine enough to explore the latitudinal structure of the ozone seasonal cycle and its radiative effects (see [section 3b](#)).

We extract monthly mean seasonal cycles of temperature, water vapor, and ozone from *Aura* MLS data at each horizontal and vertical location. We define the amplitude of each seasonal cycle as the absolute range between the seasonal cycle minimum and maximum (i.e., the “peak to peak” amplitude at monthly temporal resolution). Note that the quasi-biennial oscillation (QBO) is also an important driver of stratospheric variability (e.g., [Schoeberl et al. 2008](#)). To ensure that the QBO was not aliased in our

seasonal cycle, we examined the seasonal cycles of individual years with high and low QBO-index values (from [Freie Universität Berlin 2016](#)) during our period of record (2005–13). Depending on the phasing between the lower-stratospheric seasonal cycles and the QBO, differences between the easterly and westerly phases of QBO in any given month are up to ~ 3 K in temperature, 25% in water vapor, and 10% in ozone (not shown). However, we find that the annual cycle remains the prominent feature in lower-stratospheric temperature, water vapor, and ozone variability. Therefore, while the details (amplitude and phase) of stratospheric ozone and water vapor seasonal cycles vary with the QBO, our results are representative of typical seasonal cycle variability within this time period.

We define the tropics in this study as an average between the 20°S and 20°N latitude band. A recent study by [Stolarski et al. \(2014\)](#) found that asymmetrical upwelling and mixing between the Northern and Southern Hemispheres (NH and SH, respectively) leads to a larger amplitude ozone seasonal cycle in the NH (0° – 20°N) than the SH (20°S – 0°). In particular, lower-stratospheric upwelling and horizontal mixing impacts on ozone are in phase and additive in the NH tropics, whereas they are out of phase in the SH tropics. We explore the radiative impacts of such hemispheric variability in ozone's seasonal cycle in [section 3b](#).

[Figure 1](#) shows the tropical-mean MLS temperature, water vapor, and ozone seasonal cycles relative to the long-term mean (2005–13). Seasonal cycles are shown on the radiative transfer model's grid for direct comparison with radiative results (see model description in [section 2b](#)). The climatological tropical monthly mean model tropopause is shown as the white-dashed curve for reference.

In the tropical lower stratosphere the observed seasonal cycles of temperature, ozone, and water vapor are approximately in phase because of their common origins in anomalous seasonal upwelling. The tropical-mean amplitude of observed seasonal temperature oscillations maximizes with a ~ 7 -K amplitude at the 85-hPa level ([Fig. 1a](#)). Ozone has a very shallow tape recorder-like signal stretching from the upper troposphere up to about 50 hPa ([Fig. 1b](#)), as noted by [Randel et al. \(2007\)](#). Above the tropical tropopause, ozone's tropical-mean seasonal amplitude ranges from about 40% of the mean at 100 hPa to 17% of the mean at 53 hPa. Between 53 hPa and the upper stratosphere, ozone and temperature show a similar SAO pattern that propagates downward in time (e.g., [Hirota 1980](#); [Reid 1994](#)). Throughout the stratosphere, the water vapor structure matches the typical tropical tape recorder signal, maximizing near the annual-mean tropopause level (~ 100 hPa) with a tropical-mean amplitude of about half of the mean. Next, we use the water vapor and ozone

seasonal cycle structures to perturb a radiative transfer model and determine radiative impacts.

b. Radiative transfer calculations

For radiative calculations we employ the Parallel Offline Radiative Transfer model (PORT; Conley et al. 2013). PORT is an offline broadband radiative transfer configuration of the Community Atmosphere Model, version 4 (CAM4), in the Community Earth System Model (CESM). Gilford et al. (2016) compared PORT with a line-by-line radiative transfer model and found good agreement for both water vapor and ozone perturbations. PORT's background heating rates are similar to those of previous studies (e.g., Gettelman et al. 2004; Fueglistaler and Fu 2006; Abalos et al. 2012), though there are some differences likely associated with radiative code and constituent backgrounds (see supplemental Fig. S1). PORT has been shown to behave with accuracy similar to other broadband radiative transfer models (Gilford et al. 2016, their appendix C).

PORT is run on a $1.9^\circ \times 2.5^\circ$ horizontal grid, and has 26 vertical hybrid pressure-sigma levels between the 996 and 3 hPa. At and above the tropical tropopause, hybrid coordinates are nearly identical to pressure levels. PORT background climatology is drawn from a near-present-day (fixed at the year 2000) CESM simulation. Above the tropopause we replace the climatological backgrounds of water vapor and ozone with *Aura* MLS annual concentrations averaged over 2005–13. Radiative calculations are all sky; clouds, aerosols, other radiatively active constituents (e.g., carbon dioxide, nitrous oxide), and the monthly and spatially varying model tropopause, are fixed at year 2000 CESM climatology. In this study, PORT simulations are run for 16 months, with a 4-month spinup period followed by a 12-month analysis period. Further descriptions of PORT radiative calculations can be found in Conley et al. (2013), Neale et al. (2010), and Gilford et al. (2016, their section 3 and appendix B).

Because water vapor and ozone radiative impacts can depend on the location of the tropopause (Forster et al. 1997; Solomon et al. 2010), we use a methodology similar to that in Gilford et al. (2016) to preserve the distribution of water vapor and ozone seasonal cycles relative to the tropopause. We convert *Aura* MLS pressure coordinates to a vertical grid of log-pressure height relative to the *Aura* MLS cold-point tropopause, and then interpolate constituent concentrations onto a PORT vertical grid of log-pressure height relative to its tropopause (white dashed curves in Figs. 1 and 2). The *Aura* MLS cold-point tropopause is estimated as the coldest level in a given temperature profile; this estimate compares well with estimates from higher vertical

resolution GPS occultation measurements (e.g., Kim and Son 2012; Randel and Wu 2015). The above method is implemented monthly at each horizontal location to preserve the spatial and temporal structures of seasonal cycle perturbations.

PORT assumes seasonally evolving fixed-dynamical heating (SEFDH; Forster et al. 1997) to calculate the radiative responses of heating rates and temperatures to the seasonal cycles of water vapor and ozone. These temperature changes are referred to as “temperature adjustments.” The fixed-dynamical heating approach has been commonly used in studies of lower-stratospheric radiative temperature adjustments and radiative forcing (e.g., Forster et al. 2007; Maycock et al. 2014; Grise et al. 2009; Solomon et al. 2010; Gilford et al. 2016). Dynamical forcing is the leading cause of composition and temperature seasonal cycles in the tropical lower stratosphere (see section 1), and SEFDH assumes that the temperature seasonal cycle is primarily driven by dynamics with a fixed seasonal cycle (Forster et al. 1997). In reality a percentage of seasonal radiative heating perturbations from constituent seasonal cycles may be balanced by amplification or damping of upwelling rather than changes in temperature (e.g., Ming et al. 2016). A limitation of the SEFDH method, therefore, is that computed temperature adjustments are an upper bound on how radiative heating impacts temperatures.

Fueglistaler et al. (2011) previously applied SEFDH to explore the radiative impacts of water vapor and ozone seasonal cycles on lower-stratospheric temperatures. Chae and Sherwood (2007) instead used a radiative-convective model including an imposed seasonal cycle of residual vertical velocity to study radiative seasonal cycle effects. Both studies consistently showed that ozone significantly amplified the temperature seasonal cycle in the tropical lower stratosphere by 2–3 K. Taken together, these studies suggest that seasonal variations in ozone heating will be realized in the lower stratosphere's temperature seasonal cycle, and that to first order SEFDH is a good approximation for these effects. SEFDH is therefore a useful formulation for our purpose of bracketing and describing the radiative impacts of constituent seasonal cycles. Irrespective of potential limitations of the SEFDH formulation (excepting longwave Planck feedbacks associated with ozone heating, see discussion in section 3 and supplemental Fig. S2), changes in radiative heating rates associated with the ozone and water vapor seasonal cycles will be important for the lower-stratospheric heating budget.

We perform radiative experiments by applying three-dimensional seasonal cycles of water vapor and ozone as perturbations to the background climatology, and then run PORT assuming SEFDH. The pure radiative

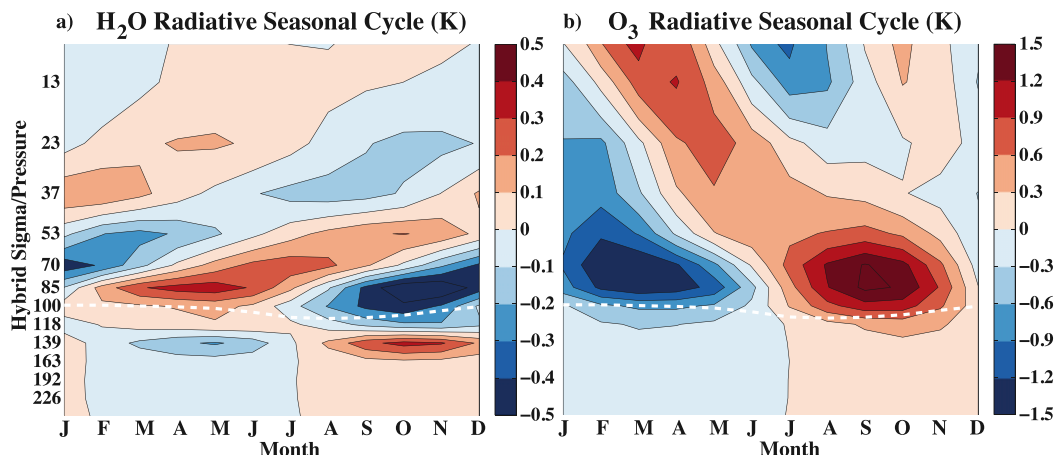


FIG. 2. Vertical structure of radiative temperature adjustments (K) associated with observed (a) water vapor and (b) ozone seasonal cycles (see Fig. 1), averaged between 20°S and 20°N. Contour intervals are 0.1 K in (a) and 0.3 K in (b). The white dashed curve denotes the PORT tropopause averaged between 20°S and 20°N.

temperature adjustments associated with these perturbations are hereafter referred to as “radiative seasonal cycles.” Following Gilford et al. (2016), temperatures are allowed to adjust up to 400 hPa below the tropopause level. Water vapor and ozone seasonal cycle perturbations (illustrated in Fig. 1) are applied between the tropopause and top of the model (~3 hPa); we refer to the output of these runs as the “full structure” radiative seasonal cycles.

To test the dependence of radiative impacts of the vertical structures of water vapor and ozone seasonal cycles, we also perform sensitivity experiments with seasonal cycle perturbations applied only between the tropopause and three vertical levels: 53, 70, and 85 hPa (i.e., a thin layer right above the tropopause). For example, in the 85-hPa sensitivity experiment, three-dimensional concentration perturbations from the seasonal cycles of water vapor and ozone are applied between the tropopause and PORT’s 85-hPa level (yellow line in Fig. 1c). Above the 85-hPa level in this sensitivity experiment, ozone and water vapor concentrations remain at their climatological average values (i.e., they have no seasonal cycles). Sensitivity experiments with larger vertical ranges were performed and found to be qualitatively consistent with those presented here (not shown for brevity).

Water vapor and ozone seasonal cycle perturbations are applied independently from one another in each run. Because of minimal spectral overlap between water vapor and ozone, their radiative seasonal cycles are approximately linearly additive. Test runs showed that the difference between the sum of the temperature adjustments associated with independent tropical-mean water vapor and ozone perturbations, and temperature adjustments

when water vapor and ozone perturbations are applied nonlinearly, is everywhere <0.02 K (not shown).

We apply seasonal cycle perturbations at and above the tropopause, as in previous studies (Grise et al. 2009; Solomon et al. 2010; Maycock et al. 2011, 2014; Gilford et al. 2016). However, radiative effects are vertically coupled (as we show in section 3b) and seasonal cycles at levels below the tropopause may also impact temperatures above the tropopause. Accordingly, we also performed runs where constituent seasonal cycles down to five vertical model levels below the tropopause (~6 km) were included as radiative perturbations. The key results from these runs are as follows: 1) temperature adjustments are qualitatively similar to those when only perturbations above the tropopause are considered; increasing the depth of seasonal cycle perturbations expands the regions of local and nonlocal temperature adjustments in the upper troposphere; 2) ozone seasonal cycles below the tropopause have small absolute amplitudes (<70 ppbv) and smaller impacts on lower-stratospheric temperatures than ozone seasonal cycles above the tropopause (consistent with the findings of Forster et al. 2007); 3) the radiative response of upper-tropospheric water vapor is largest in the tropopause region, and is therefore very sensitive to the location of the tropopause (consistent with Forster et al. 1997; Solomon et al. 2010; Gilford et al. 2016). However, these effects are local to the immediate tropopause levels (between 85 and 118 hPa); consistent local temperature adjustments associated with the water vapor seasonal cycle fall off sharply below 118 hPa. We therefore choose to restrict our analyses in the following section to results with perturbations considered only above the tropopause.

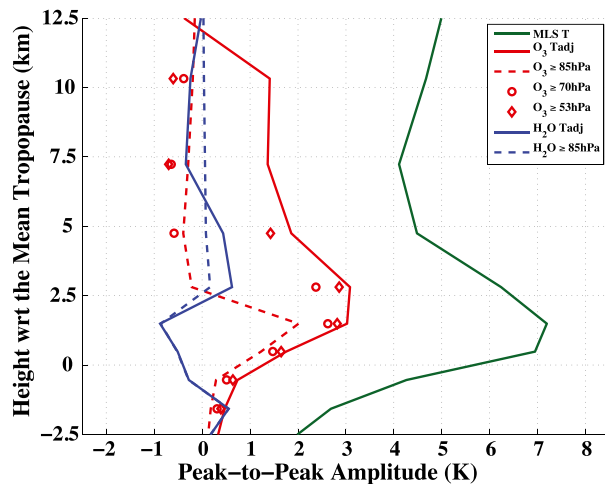


FIG. 3. The peak-to-peak seasonal cycle amplitudes (K) relative to the tropopause height (log-pressure km) of observed MLS temperature (green curve), ozone and water vapor radiative temperature adjustments (Tadj) associated with seasonal cycles between the tropopause and the top of the stratosphere (red and blue solid curves, respectively), ozone and water vapor radiative temperature adjustments associated with seasonal cycles considered between the tropopause and 85 hPa (red and blue dashed curves, respectively), and ozone radiative temperature adjustments associated with seasonal cycles considered between the tropopause and 70 hPa (red circles) and 53 hPa (red diamonds). All amplitudes are averaged between 20°S and 20°N. Positive amplitudes represent potential amplification of the temperature seasonal cycle (i.e., the maxima occurs in summer/fall), while negative amplitudes represent potential damping of the temperature seasonal cycle (i.e., the maxima occurs in winter/spring).

3. Results

a. Full structure temperature adjustments and heating rates

The tropical-mean seasonal cycles of temperature adjustments associated with the full structures of water vapor and ozone seasonal cycles (i.e., the “radiative seasonal cycles”) are shown in Fig. 2. The tropical-mean peak-to-peak amplitudes (in K) of the MLS observed temperature seasonal cycle, the water vapor radiative seasonal cycle, and the ozone radiative seasonal cycle are shown in Fig. 3 relative to the annual-mean tropopause height (along with sensitivity experiments discussed in section 3b). Positive amplitudes in Fig. 3 show where the radiative seasonal cycles have a similar phase to the temperature seasonal cycle at that altitude (e.g., lower-stratospheric ozone and temperature minimizing in boreal winter/spring and maximizing in boreal summer/fall); negative amplitudes show where radiative seasonal cycles have a phase opposite to the temperature seasonal cycle at that altitude. Seasonal cycle radiative adjustments represent the upper bound on ozone and water vapor

radiative contributions to amplifying (in the case of ozone) or damping (in the case of water vapor) stratospheric temperature seasonal cycles.

Radiative adjustments (Fig. 2) lag seasonal cycle perturbations (Fig. 1) by 1–2 months in the tropical lower stratosphere. This lag is associated with the seasonal heating rate anomalies (i.e., temperature adjustments maximize when heating rate anomalies transition from positive to negative or vice versa, see Fig. 4) and is on the order of the thermal radiative damping time scales near the tropical tropopause (Newman and Rosenfield 1997; Randel et al. 2002a; Gettelman et al. 2004; Randel and Wu 2015). In the tropical lower stratosphere there are significant correlations between temperature, water vapor, and ozone primarily through upwelling and thermodynamics (e.g., Gilford et al. 2016). The lower-stratospheric radiative time lag therefore implies that radiative contributions to the temperature seasonal cycle should act to shift its phase (consistent with Chae and Sherwood 2007). The phase shift implies that amplifying or damping effects will have a smaller effect on the total amplitude of lower-stratospheric temperatures than they would if there was no time lag, particularly for water vapor contributions (discussed below). However, radiative contributions from ozone and water vapor still remain important terms in the *overall* budgets of lower-stratospheric seasonal cycles of temperatures and heating rates.

The tropical-mean full structure of the water vapor radiative seasonal cycle (Fig. 2a) shows radiative adjustments that maximize just above the tropopause (~ 85 hPa) with a range of 0.9 K, and then propagate upward into the stratosphere: a radiative tape recorder effect. Above the tropopause, water vapor’s radiative seasonal cycle is consistent with its role of net cooling to space (Gettelman et al. 2004): reductions in water vapor lead to net warming in the boreal winter/spring, whereas increases in water vapor lead to net cooling in the boreal summer/fall. If these purely radiative adjustments were linearly removed from the temperature seasonal cycle, the seasonal temperature amplitude at 85 hPa would be increased by ~ 0.2 K (about 3%). Because of the phase offset between temperature and water vapor’s radiative seasonal cycle, water vapor’s radiative effect acts to shift the temperature seasonal cycle toward earlier annual extrema. Water vapor’s radiative seasonal cycle maximizes in the lower stratosphere both because (i) it is the location of water vapor’s maximum seasonal cycle amplitude (Fig. 1b) and because (ii) it is the location of maximum radiative sensitivity to tropical water vapor perturbations (e.g., Forster and Shine 1999; Solomon et al. 2010).

Below the tropical tropopause, the radiative response to the tropical water vapor tape recorder switches sign:

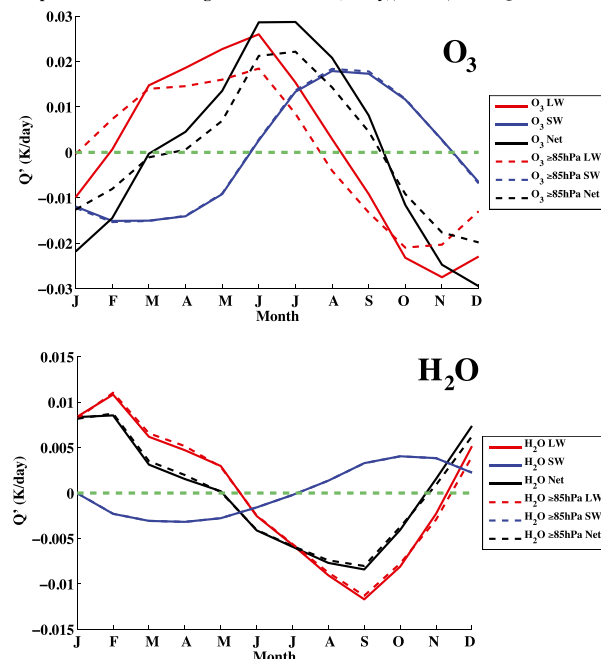
Tropical Radiative Heating Rate Anomalies (K/day), 85hPa, mean $Q = 0.33$ K/day

FIG. 4. Seasonal cycles of calculated radiative heating rate anomalies ($K\ day^{-1}$) from the climatological average heating rates, averaged between $20^{\circ}S$ and $20^{\circ}N$ on the 85-hPa level. Heating rate anomalies are associated with the seasonal cycles of (top) ozone and (bottom) water vapor. Heating rates are separated into longwave (red curves), shortwave (blue curves), and net (black curves) components. Solid curves show the heating rates obtained when the constituent seasonal cycles are considered throughout the stratosphere (from the tropopause to model top, ~ 3 hPa). The heating rates obtained when constituent seasonal cycles are considered only between the tropopause and 85 hPa are shown with the dashed curves. The green dashed curve in each panel denotes $0\ K\ day^{-1}$, where heating rates pass from positive (converging toward warmer temperatures) to negative (converging toward cooler temperatures), or vice versa. For reference, the annual-mean heating rate at 85 hPa is shown in the figure title.

there is net cooling in the boreal winter/spring, net warming in the boreal summer/fall, and near-zero temperature adjustments across the tropopause level itself. This is consistent with previous studies of the radiative effects of lower-stratospheric water vapor anomalies (e.g., Gilford et al. 2016). Physically, an opposite-signed radiative effect in the upper troposphere arises because of (i) changes in the amount of longwave radiation propagating down through the tropopause (which scale with water vapor concentration), and (ii) changes in the lower stratosphere opacity (allowing the layers below to transmit longwave radiation and cool more or less efficiently to space).

The tropical-mean radiative seasonal cycle associated with ozone's full structure shows radiative adjustments that maximize at ~ 70 – 85 hPa (Fig. 3). Ozone

perturbations drive changes in shortwave absorption that strongly affect local temperature, and in turn lead to changes in longwave emission through a Planck feedback (Ramanathan and Dickinson 1979; Gettelman et al. 2004; Grise et al. 2009; Gilford et al. 2016). The SEFDH methodology enables exploration of the Planck feedback (its impacts on ozone's tropical lower-stratospheric radiative heating are explicitly shown in supplemental Fig. S2). The net radiative effect of ozone's seasonal cycle is to cool the tropical lower stratosphere in the boreal winter/spring and warm the tropical lower stratosphere in the boreal summer/fall. The amplitude of ozone's radiative seasonal cycle at 85 hPa is about 3 K ($\sim 31\%$ of the *Aura* MLS temperature amplitude at that altitude).

Changes in tropical lower-stratospheric ozone's longwave propagation also result in a radiative seasonal cycle below the tropopause that cools upper-tropospheric temperatures in the boreal winter/spring and warms them in the boreal summer/fall (Ramanathan and Dickinson 1979; Grise et al. 2009). Shortwave heating from changes in the penetration of solar radiation slightly damps the longwave effect (not shown). Ozone's radiative seasonal cycle in the upper troposphere falls off sharply with depth: the 1.75-K seasonal cycle range near the tropopause is reduced to about 0.5 K at 139 hPa. In the upper troposphere, water vapor radiative effects are same signed and approximately in phase with ozone effects, leading to the sum of their radiative seasonal cycle amplitudes at 139 hPa being about 1 K. Water vapor effects between 139 hPa and the tropopause are smaller because it is the crossover (near-zero adjustment) region between local stratospheric effects and nonlocal upper-tropospheric effects, while nonlocal ozone effects continue to fall off below this level. Therefore, there is a specific vertical region in the upper troposphere where both the overlying stratospheric water vapor and ozone are significant contributors to a radiative seasonal cycle.

Fueglistaler et al. (2011) found that the seasonal ozone radiative response in the lower stratosphere (67-hPa level) was an order of magnitude larger than the water vapor response. In this study we find that the amplitude of the tropical-mean ozone radiative seasonal cycle at 70 hPa is ~ 5 times larger than the water vapor seasonal cycle (~ 3.1 vs ~ -0.6 K). However, it is clear from Figs. 2 and 3 that the water vapor radiative seasonal cycle maximizes at altitudes below the 70-hPa level, whereas the ozone radiative seasonal cycle maximizes more broadly over ~ 70 – 85 hPa. This is likely because of (i) water vapor's strong radiative sensitivity to the tropopause altitude (e.g., Solomon et al. 2010), and (ii) the amplitude of ozone's concentration seasonal cycle is

larger at higher altitudes. At the two levels just above the annual-mean tropopause (85 and 100 hPa), the tropical-mean ozone radiative seasonal cycle is ~ 3.4 times larger than the water vapor radiative seasonal cycle (~ 3 vs ~ -0.9 K, and ~ 1.75 vs ~ -0.5 K, respectively, Fig. 3). Therefore at near-tropopause levels we find that water vapor seasonal radiative effects are small compared with ozone, but not negligible.

Figure 4 shows the seasonal cycles of computed lower-stratospheric heating rate anomalies (from the climatological background heating rates) associated with ozone and water vapor seasonal cycles. For comparison, the absolute value of the annual-mean net heating rate at 85 hPa is 0.33 K day^{-1} (see supplemental Fig. S1). PORT-computed radiative heating rates in the tropical lower stratosphere have similar seasonal cycles and absolute magnitudes to those of Abalos et al. (2012), though there are some differences likely related mainly to seasonal cycle depictions and background climatology.

We find that ozone's lower-stratospheric radiative temperature amplification is a mixture of longwave and shortwave effects (consistent with Forster et al. 2007) that have different phases but result in net warming rates from April to August and net cooling rates from September to March (Fig. 4). Shortwave effects follow ozone seasonal cycle concentrations, while longwave effects are modulated by a nearly linear combination of the radiation (i) following ozone concentrations, and (ii) tracking increases or decreases in local temperature adjustments (Planck feedback, see supplemental Fig. S2). The net ozone radiative heating rate anomaly amplitude at 85 hPa is $\sim 0.06 \text{ K day}^{-1}$, of similar magnitude to the ozone heating rate seasonal cycle amplitude found at 17 km (~ 90 hPa) by Folkins et al. (2006, see their Fig. 4), although our calculations are adjusted rather than instantaneous heating rates.

Observational estimates of lower-stratospheric dynamical cooling through tropical upwelling by Abalos et al. (2012) are of comparable magnitude to radiative heating and vary inversely, driving seasonal temperature tendencies in the tropical lower stratosphere toward 0 K day^{-1} (see also Rosenlof 1995). The amplitude of the seasonal cycle of the dynamical cooling at 80 hPa is about 0.2 K day^{-1} (Abalos et al. 2012, see their Fig. 5). The ozone seasonal cycle radiative heating anomalies (Fig. 4) share a similar phase with adiabatic cooling anomalies (minimum heating in boreal winter and maximum in boreal summer), and ozone's radiative heating amplitude is about a third of the dynamical seasonal amplitude. Because of its relative magnitude, we conclude that ozone radiative heating is an important term in the seasonal heating budget and acts to amplify the seasonal cycle of lower-stratospheric temperatures. This agrees well with our

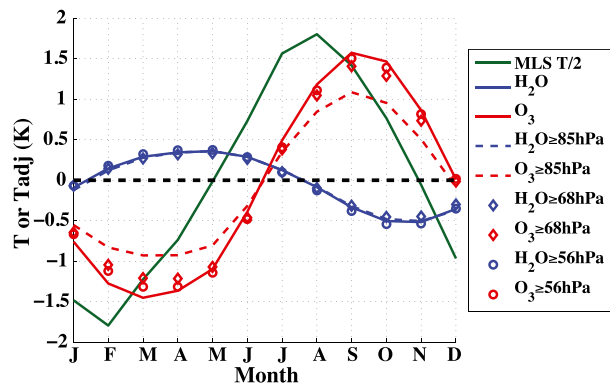


FIG. 5. Seasonal cycles of MLS observed temperatures divided by 2 (green curve), and the temperature adjustments associated with the observed seasonal cycles in water vapor (blue curves/symbols) and ozone (red curves/symbols) on the 85-hPa pressure level and averaged between 20°S and 20°N . The solid curves show the radiative seasonal cycles obtained when the constituent seasonal cycles are considered throughout the stratosphere (from the tropopause to model top, ~ 3 hPa). Radiative seasonal cycles obtained when constituent seasonal cycles are considered only between the tropopause and 85 hPa are shown with the dashed curves. Likewise for constituent seasonal cycles considered between the tropopause and 70 hPa (diamonds), and 53 hPa (circles).

comparison between temperature adjustments and observed temperatures (with temperature adjustments at 85 hPa having an amplitude that is $\sim 31\%$ of the MLS observed temperature amplitude), and the previous findings of Chae and Sherwood (2007) and Fueglistaler et al. (2011).

Water vapor seasonal cycles of shortwave and longwave heating rates in the lower stratosphere have opposing signs (e.g., Gettelman et al. 2004) with longwave radiation being the larger term. The competing effects result in net cooling in the boreal summer and warming in the boreal winter (an amplitude of a little less than $\sim 0.02 \text{ K day}^{-1}$ at 85 hPa). We conclude that while water vapor's seasonal radiative effects near the tropical tropopause are not negligible [in contrast to Folkins et al. (2006) who found no seasonal water vapor radiative signal at ~ 90 hPa], they are about a third of those associated with ozone.

b. Sensitivity experiments and latitudinal variability

We now explore the importance of overlying seasonal cycle structures for lower-stratospheric radiative seasonal cycles. Figure 5 shows the radiative seasonal cycles of water vapor and ozone on the 85-hPa level associated with full structure experiments and the 85-, 70-, and 53-hPa sensitivity experiments. The MLS observed seasonal cycle of temperature anomalies (divided by 2 for scale) is also shown in Fig. 5 for comparison with the radiative seasonal cycles. MLS temperature seasonal cycle anomalies minimize in February (~ -3 K) and

maximize in August (~ 4.5 K) with a total amplitude of ~ 7.5 K. For reference, Fig. 3 also shows the tropical-mean peak-to-peak amplitudes of full structure experiments versus select sensitivity experiments.

At 85 hPa the water vapor radiative seasonal cycle associated with the full vertical structure of perturbations (solid blue curve) is very similar to the radiative seasonal cycles when changes above 85 (dashed blue curve), 70 (blue diamonds), or 53 hPa (blue circles) are not considered (there is $<10\%$ difference, <0.1 K, between the amplitudes of any of their radiative cycles). This result indicates that the radiative effect of water vapor's seasonal cycle on the temperature seasonal cycle at 85 hPa is almost entirely local, and is insensitive to the vertical structure of overlying water vapor anomalies. While this result is consistent in the context of the water vapor radiative kernel function maximum at near-tropopause levels (e.g., Solomon et al. 2010), the radiative seasonal cycle was not constrained to be strictly local. The lack of overlying effects demonstrates that understanding what sets the seasonality of water vapor concentrations right at the tropical tropopause level is the most important factor in determining water vapor's lower-stratospheric seasonal radiative effects. Comparison with the amplitudes in Fig. 3 shows that the radiative effect of water vapor between the tropopause and 85 hPa falls off to near zero in the layers above 85 hPa, missing the canonical tape recorder structure evident in full structure calculations. Given the smaller magnitude of water vapor radiative seasonal cycle in the lower stratosphere and its lack of vertical structure sensitivity, we focus the remainder of our analysis on the ozone radiative seasonal cycle.

An important finding of this study is that, in contrast to water vapor, ozone's seasonal radiative effects in the lower stratosphere are sensitive to nonlocal overlying changes in ozone. The deviations between radiative seasonal cycles associated with ozone's full vertical structure and the sensitivity experiments (Figs. 3 and 5) indicate that the amplitude of ozone's radiative seasonal cycle at 85 hPa depends on both local and nonlocal ozone changes. By considering perturbations between the tropopause and the 85- or 70-hPa levels, for instance, only $\sim 66\%$ or $\sim 87\%$ (respectively) of the full radiative seasonal cycle amplitude is recovered (amplitude differences of ~ 1 and 0.4 K, respectively). To capture $>90\%$ of the full radiative seasonal cycle amplitude, the ozone seasonal cycles up to ~ 50 hPa or above must be considered. Overlying stratospheric ozone anomalies are therefore important for seasonal lower-stratospheric radiative impacts. Accordingly, simulating ozone's seasonal radiative influences on lower-stratospheric temperatures and dynamics requires ozone anomalies both near and away from the tropopause to be well depicted. Further,

future long-term trends in the seasonal cycles of tropical lower- and middle-stratospheric ozone should be significant for the future evolution of the near-tropopause diabatic heat budget and temperatures (e.g., Forster et al. 2007; Polvani and Solomon 2012).

Heating rate anomalies show that ozone sensitivities to the overlying vertical structure are related to changes in longwave heating (Fig. 4). When seasonal cycles above 85 hPa are not considered in the sensitivity experiment (red dashed curve, top panel of Fig. 4), the radiative seasonal amplification of temperatures in the layers above 85 hPa disappears (in fact these seasonal cycles damp slightly, see the dashed red curve in Fig. 3), reducing these layers' transmission of nonlocal Planck feedbacks to the 85-hPa level. The damped overlying temperature seasonality combined with the lack of overlying ozone concentration seasonality damps the longwave heating at 85 hPa, driving ozone's vertical structure sensitivity shown in Figs. 3 and 5. Shortwave contributions to the 85-hPa ozone radiative seasonal cycle (blue curves, top panel of Fig. 4) are local to the layer between the tropopause and 85 hPa to within $<1\%$.

The latitudinal structure of the area-weighted (multiplied by the cosine of latitude) ozone radiative seasonal cycle at 85 hPa is shown in Fig. 6b. Temperature adjustments from the full vertical structure of the ozone seasonal cycle are shown, along with temperature adjustments when considering only the ozone seasonal cycle between the tropopause and 85 hPa (i.e., the 85-hPa sensitivity experiment) minus the temperature adjustments from the full vertical structure experiment. Contours overlying shading of opposite sign indicate where excluding the ozone seasonal cycle above 85 hPa damps the amplitude of the ozone radiative seasonal cycle at 85 hPa (cf. Fig. 5). For reference, Fig. 6a shows the latitudinal structure of *Aura* MLS area-weighted ozone seasonal cycles on the 85-hPa surface. The full range of results from 75°S to 75°N is shown for comparison with Fueglistaler et al. (2011, see their Fig. 5); the yellow lines in Fig. 6b denote the tropical region specifically considered in this study. The full structure of the radiative seasonal cycle in Fig. 6 is qualitatively consistent with that in Fueglistaler et al. (2011, see their Fig. 5b) at 67 hPa, but further elucidates the spatial structure of the lowermost stratosphere's sensitivity to overlying ozone seasonal cycles. To clarify the differences between the two hemispheres, Fig. 7 shows the observed ozone seasonal cycles and their associated full structure radiative seasonal cycles averaged between the SH tropics (20°S – 0° , Figs. 7a and 7c) and the NH tropics (0° – 20°N , Figs. 7b and 7d).

Just above the tropopause in the NH tropics (0° – 20°N), the full vertical structure ozone radiative seasonal cycle

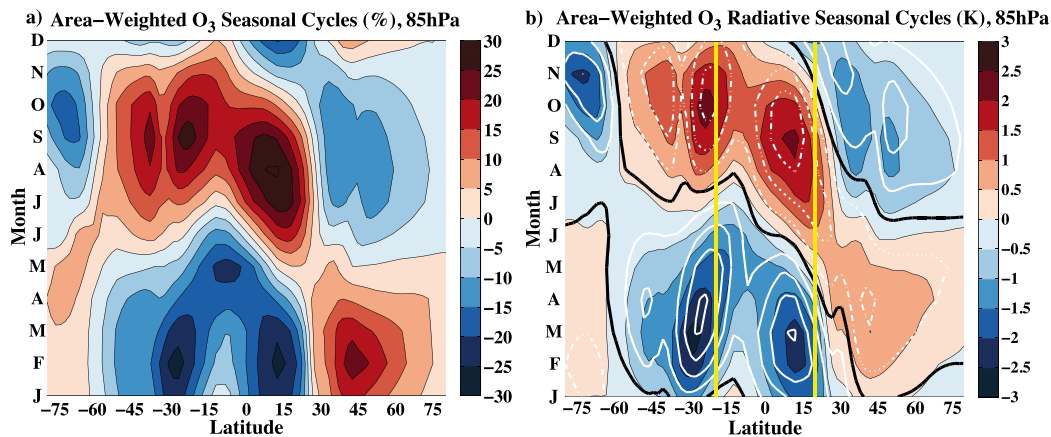


FIG. 6. (a) The area-weighted ozone seasonal cycle on the 85-hPa pressure level (%); the contour interval is 5%. (b) Colored shading shows the area-weighted latitudinal structure of temperature adjustments, on the 85-hPa pressure level, obtained when the full structure of the ozone seasonal cycle is considered throughout the stratosphere (from the tropopause to model top, ~ 3 hPa). The shading contour interval is 0.5 K. White contours show the area-weighted temperature adjustments obtained when the ozone seasonal cycles is considered only between the tropopause and 85 hPa minus the temperature adjustments obtained when considering the full structure (i.e., the shading). Positive (negative) differences are denoted with solid (dash-dot) white lines. The bold black line is the 0-K contour line for the differences. The white contour interval is 0.2 K. The yellow lines denote the tropical range from 20°S to 20°N.

has a maximum amplitude at $\sim 12^\circ\text{N}$, with maximum radiative cooling (adjustments of ~ -2.2 K) between February and March, and maximum radiative warming (adjustments of ~ 2.2 K) in September (Fig. 6). The amplitude averaged between 0° and 20°N is about 3.8 K. When ozone perturbations above 85 hPa are not considered, the amplitude of the NH tropical ozone radiative seasonal cycle is reduced by $\sim 35\%$. There is only a ~ 1 -month phase shift in the NH ozone radiative seasonal cycle when seasonal cycles above the 85-hPa level are not considered (Fig. 6), because the ozone seasonal cycle in the NH tropics is nearly in phase between 100 and 50 hPa (Fig. 7b).

The SH radiative seasonal cycle (ranging between 20°S and 0°) associated with the full vertical structure of the ozone seasonal cycle has a smaller amplitude than the NH tropics (3 vs 3.8 K) and is less homogenous across the SH tropical band (Fig. 6). The maximum radiative cooling is found in April, ranging from -1.8 K at 20°S to -1 K at 10°S . The maximum radiative warming is found in October, ranging from 2.3 K at 20°S to 1.2 K at 10°S . This result is consistent with Stolarski et al. (2014), who emphasized that the tropical lower-stratosphere ozone seasonal cycle is smaller in the SH than the NH, and SH seasonal cycle lags the NH cycle by 1–2 months (cf. Figs. 6a and 7a,b). At latitudes between the equator and 15°S , there is less sensitivity to overlying changes than in the NH tropics; the radiative seasonal cycle averaged over this range is damped by only $\sim 27\%$ when contributions from the ozone seasonal cycle above

85 hPa are not considered (cf. $\sim 35\%$ damping in the NH tropics), and phase changes are also small. The SH tropical (20°S – 0°) ozone seasonal cycle (Fig. 7a) and the associated full structure radiative seasonal cycle (Fig. 7c) are shallower than those of the NH (Figs. 7b and 7d), contributing to the reduced radiative sensitivity to seasonality above 85 hPa.

At higher southern latitudes largely outside the traditional tropical band, there is a strong ozone concentration and radiative seasonal cycle on the 85-hPa level stretching from 35° to 15°S (Fig. 6). This feature arises because of the migration of the tropical region on the 85-hPa pressure surface, moving northward in the boreal summer and southward in the austral summer (Stolarski et al. 2014). Strong upwelling and weak horizontal in mixing across the subtropical jet promotes reductions in ozone at these latitudes from January to March (Chen 1995; Stolarski et al. 2014). As the tropical lower stratosphere retreats northward in the boreal summer, it is replaced in this region by extratropical air with higher concentrations of ozone. The result is a consistent strong seasonal cycle of ozone that is in phase between the tropopause and ~ 50 hPa, with large seasonal cycle amplitudes between 50% and 23%, respectively (see supplemental Fig. S3). Because the overlying seasonal cycles are in phase with the cycles below (see supplemental Fig. S3), the local and non-local radiative effects compound and lead to a radiative seasonal cycle that maximizes at $\sim 24^\circ\text{S}$ with an amplitude of 4.9 K. When the seasonal cycle above

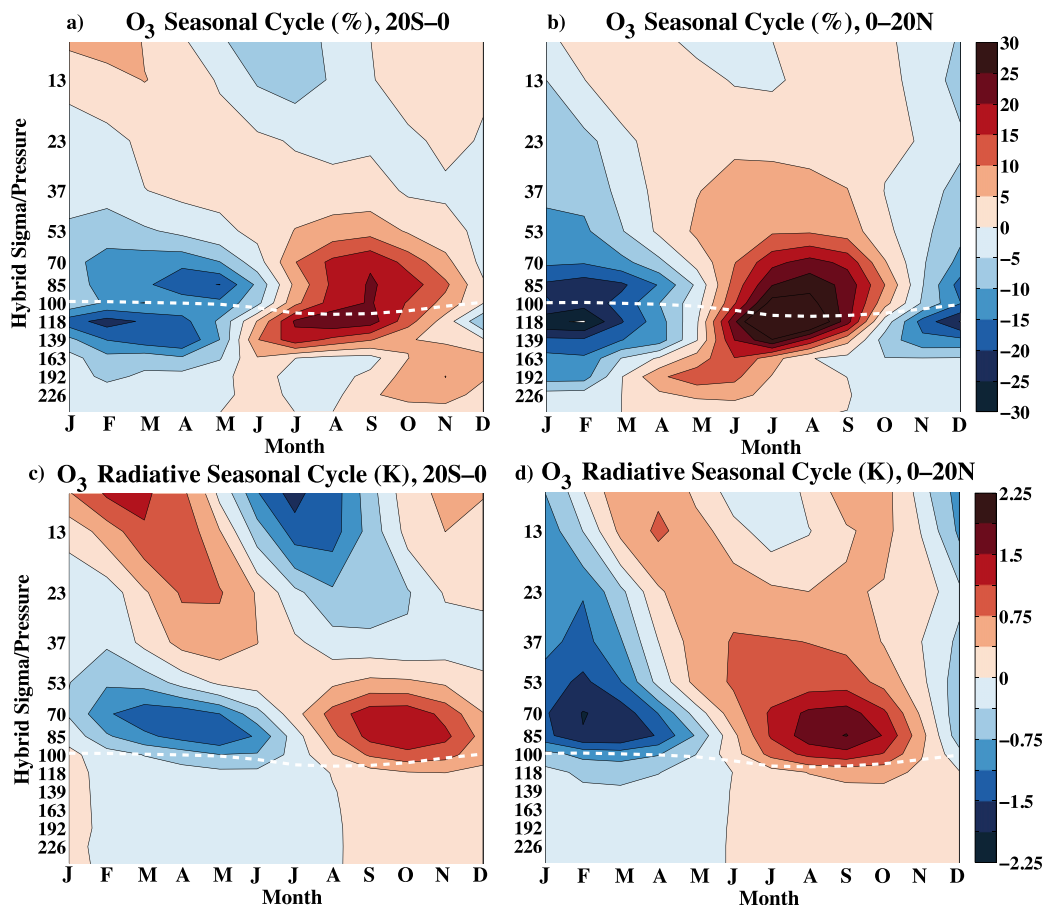


FIG. 7. (a),(b) As in Fig. 1c, but for ozone observations averaged between (a) 20°S–0° and (b) 0°–20°N. The contour interval is 5%. (c),(d) As in Fig. 2b, but for radiative temperature adjustments associated with ozone averaged between (c) 20°S–0° and (d) 0°–20°N. The contour interval is 0.375 K. The white dashed curve in each figure denotes each region's PORT climatological tropopause.

85 hPa is not considered, the average amplitude of the radiative seasonal cycle between 35° and 15°S at 85 hPa is reduced to about 3.1 K (a 26% reduction from the full structure ozone radiative seasonal cycle). While these changes are physical, they are only relevant for the tropical lower stratosphere during the austral summer months when the SH tropics extend to these latitudes.

The distinct horizontal patterns in NH and SH ozone, related to the increased mixing in the NH surf-zone region, the migration of the tropical lower stratosphere, and the phasing of upwelling and horizontal mixing in the two hemispheres (Stolarski et al. 2014), result in meridionally asymmetric radiative effects in the tropics. When considering the impacts of radiative effects on lower-stratospheric or near-tropopause phenomena in detail (such as the outflow of tropical cyclones or the amount of water vapor entering the stratosphere), the latitudinal variability examined here should be taken

into account. Notably, seasonal cycle amplitudes of tropical lower-stratospheric temperatures maximize in the NH tropics (Reed and Vlcek 1969; Randel et al. 2003; Fueglistaler et al. 2009a; Grise and Thompson 2013). Our results indicate that the ozone radiative effects amplify this hemispheric asymmetry.

4. Summary

This study used *Aura* Microwave Limb Sounder (MLS) observations of tropical stratospheric water vapor and ozone and a radiative transfer model to determine their purely radiative impacts on the upper troposphere and lower stratosphere. The radiative sensitivities to the specific vertical structures of water vapor and ozone seasonal cycles were investigated to ascertain how overlying seasonal cycles nonlocally impact radiative temperature adjustments in the lower stratosphere. Hemispheric asymmetries in ozone's

seasonal radiative effects and sensitivities were also elucidated.

The key findings of this study are as follows:

- 1) Ozone's seasonal radiative effect is broad across the tropical lower stratosphere, whereas water vapor's seasonal radiative effect maximizes just above the tropopause. Ozone is the larger contributor to the seasonal radiative impacts in the tropical lower stratosphere—at levels just above the tropical tropopause, ozone's seasonal cycle of radiative temperature adjustments has a peak-to-peak amplitude that is ~ 3.4 times that of water vapor—but water vapor's seasonal radiative effects are more influential than was previously thought, suggesting that neglecting water vapor seasonality when considering the radiative budget of the tropical stratosphere could miss important variability (Folkins et al. 2006; Chae and Sherwood 2007; Fueglistaler et al. 2011). Water vapor's signal is about a third that of ozone primarily because of offsetting longwave and shortwave effects. Ozone's larger heating rates are the sum of shortwave effects following ozone concentrations and longwave effects following both concentrations and associated temperature adjustments (Planck feedback).
- 2) The radiative impacts of water vapor's seasonal cycle in the lower stratosphere are not sensitive to the overlying water vapor structure. That is, local radiative responses largely drive water vapor's "radiative tropical tape recorder." In contrast, $\sim 33\%$ of the radiative effects of ozone's seasonal cycle at 85 hPa are associated with longwave emission from ozone seasonal cycles overlying the 85-hPa level. To recover 90% or more of ozone's seasonal radiative response near the tropical tropopause, ozone seasonal cycles up to at least ~ 50 hPa must be included in radiative calculations. It is therefore important that ozone's nonlocal radiative effects above the lower stratosphere be accounted for when characterizing the seasonal radiative budget in the tropical lower stratosphere.
- 3) Ozone's lower-stratospheric seasonal radiative effects are asymmetric about the equator: the radiative seasonal cycle amplitude in the Northern Hemisphere tropics (0° – 20°N) is 27% larger (0.8 K) than that in the Southern Hemisphere tropics (20°S – 0°). Additionally, ozone radiative impacts in the Northern Hemisphere tropical lower stratosphere have $\sim 8\%$ greater absolute sensitivity to the overlying seasonal ozone structure than the Southern Hemisphere tropics. These results are linked to the observed asymmetrical ozone concentration seasonal cycle detailed by Stolarski et al. (2014). More work is needed to understand how ozone's radiative asymmetry about the

equator contributes to the observed meridional asymmetry in tropical lower-stratospheric temperature seasonal cycles (e.g., Randel et al. 2003).

In this study we have not assessed the seasonal radiative effects of other lower-stratospheric constituents such as nitrous oxide or methane [although these effects would likely be minor, Gettelman et al. (2004)], aerosols, or clouds, each of which could play a role in the seasonal radiative budget in the tropical lower stratosphere (e.g., Fueglistaler et al. 2009a). A further limitation of this study is the reliance on seasonally evolving fixed dynamical heating (SEFDH; Forster et al. 1997) to estimate the radiative seasonal cycles of water vapor and ozone. Whereas SEFDH is useful for determining the pure radiative temperature response to observed constituent changes in the stratosphere, it is only an upper bound estimate of radiative effects on temperature, because dynamics could to some extent respond, thus balancing seasonal anomalies in radiative heating (e.g., Ming et al. 2016). Radiative contributions to temperatures in the lower stratosphere may consequently be lower than the upper bound determined herein.

We also calculated the heating rates associated with observed water vapor and ozone seasonal cycles, which are observationally constrained and only depend on SEFDH to the extent that it is used to estimate longwave adjusted heating rates (Planck feedback). The amplitude of ozone heating rates is about a third of estimated dynamical heating rate amplitudes in the tropical lower stratosphere (Abalos et al. 2012), suggesting that ozone does substantially contribute to the seasonal heating budget and by extension the seasonal temperature budget in the tropical lower stratosphere.

As the stratospheric circulation is expected to change over this century in response to climate change (e.g., McLandress and Shepherd 2009; Fu et al. 2015), understanding the factors that impact radiative heating in the tropical lower stratosphere will be important for model and reanalysis representations of the stratosphere and tropopause. The work presented herein suggests that misrepresenting the ozone seasonal cycle in the lower stratosphere and the layers above will have consequences for seasonal radiative heating near the tropical tropopause. Along with seasonal trends in stratospheric temperatures and/or stratospheric circulation (such as those suggested by Fu et al. 2010), seasonal radiation could also change and indirectly affect physical phenomena that depend on future near-tropopause temperatures, such as the amount of water vapor entering the atmosphere or the intensity of tropical cyclones.

Acknowledgments. The lead author thanks Richard Stolarski, Bill Randel, Amanda Maycock, Bob Portmann, and Karen Rosenlof for helpful discussions that improved

this work. Thanks to Jeff Scott for his oversight of the computer cluster on which our model simulations were performed. We thank three anonymous reviewers whose suggestions improved this manuscript. DG and SS were supported by NASA headquarters under the NASA Earth and Space Science Fellowship Program by Grant NNX14AK83H and by NSF Grant AGS-1461517.

REFERENCES

- Abalos, M., W. J. Randel, and E. Serrano, 2012: Variability in upwelling across the tropical tropopause and correlations with tracers in the lower stratosphere. *Atmos. Chem. Phys.*, **12**, 11 505–11 517, doi:[10.5194/acp-12-11505-2012](https://doi.org/10.5194/acp-12-11505-2012).
- , —, D. E. Kinnison, and E. Serrano, 2013: Quantifying tracer transport in the tropical lower stratosphere using WACCM. *Atmos. Chem. Phys.*, **13**, 10 591–10 607, doi:[10.5194/acp-13-10591-2013](https://doi.org/10.5194/acp-13-10591-2013).
- Bister, M., and K. A. Emanuel, 1998: Dissipative heating and hurricane intensity. *Meteor. Atmos. Phys.*, **65**, 233–240, doi:[10.1007/BF01030791](https://doi.org/10.1007/BF01030791).
- Brasseur, G., and S. Solomon, 1986: *Aeronomy of the Middle Atmosphere*. Springer, 452 pp.
- Chae, J. H., and S. C. Sherwood, 2007: Annual temperature cycle of the tropical tropopause: A simple model study. *J. Geophys. Res.*, **112**, D19111, doi:[10.1029/2006JD007956](https://doi.org/10.1029/2006JD007956).
- Chen, P., 1995: Isentropic cross-tropopause mass exchange in the extratropics. *J. Geophys. Res.*, **100**, 16 661–16 673, doi:[10.1029/95JD01264](https://doi.org/10.1029/95JD01264).
- Conley, A. J., J.-F. Lamarque, F. Vitt, W. D. Collins, and J. Kiehl, 2013: PORT, a CESM tool for the diagnosis of radiative forcing. *Geosci. Model Dev.*, **6**, 469–476, doi:[10.5194/gmd-6-469-2013](https://doi.org/10.5194/gmd-6-469-2013).
- Dessler, A. E., M. R. Schoeberl, T. Wang, S. M. Davis, and K. H. Rosenlof, 2013: Stratospheric water vapor feedback. *Proc. Natl. Acad. Sci. USA*, **110**, 18 087–18 091, doi:[10.1073/pnas.1310344110](https://doi.org/10.1073/pnas.1310344110).
- , and Coauthors, 2016: Transport of ice into the stratosphere and the humidification of the stratosphere over the 21st century. *Geophys. Res. Lett.*, **43**, 2323–2329, doi:[10.1002/2016GL067991](https://doi.org/10.1002/2016GL067991).
- Emanuel, K., S. Solomon, D. Folini, S. Davis, and C. Cagnazzo, 2013: Influence of tropical tropopause layer cooling on Atlantic hurricane activity. *J. Climate*, **26**, 2288–2301, doi:[10.1175/JCLI-D-12-00242.1](https://doi.org/10.1175/JCLI-D-12-00242.1).
- Folkens, I., P. Bernath, C. Boone, G. Lesins, N. Livesey, A. M. Thompson, K. Walker, and J. C. Witte, 2006: Seasonal cycles of O₃, CO, and convective outflow at the tropical tropopause. *Geophys. Res. Lett.*, **33**, L16802, doi:[10.1029/2006GL026602](https://doi.org/10.1029/2006GL026602).
- Forster, P. M., and K. P. Shine, 1999: Stratospheric water vapour changes as a possible contributor to observed stratospheric cooling. *Geophys. Res. Lett.*, **26**, 3309–3312, doi:[10.1029/1999GL010487](https://doi.org/10.1029/1999GL010487).
- , R. S. Freckleton, and K. P. Shine, 1997: On aspects of the concept of radiative forcing. *Climate Dyn.*, **13**, 547–560, doi:[10.1007/s003820050182](https://doi.org/10.1007/s003820050182).
- , G. Bodeker, R. Schofield, S. Solomon, and D. Thompson, 2007: Effects of ozone cooling in the tropical lower stratosphere and upper troposphere. *Geophys. Res. Lett.*, **34**, L23813, doi:[10.1029/2007GL031994](https://doi.org/10.1029/2007GL031994).
- Freie Universität Berlin, 2016: The Quasi-Biennial Oscillation (QBO) data series. Institute of Meteorology, Freie Universität Berlin, accessed 3 June 2015. [Available online at <http://www.geo.fu-berlin.de/en/met/ag/strat/produkte/qbo/>.]
- Fu, Q., S. Solomon, and P. Lin, 2010: On the seasonal dependence of tropical lower-stratospheric temperature trends. *Atmos. Chem. Phys.*, **10**, 2643–2653, doi:[10.5194/acp-10-2643-2010](https://doi.org/10.5194/acp-10-2643-2010).
- , P. Lin, S. Solomon, and D. L. Hartmann, 2015: Observational evidence of strengthening of the Brewer–Dobson circulation since 1980. *J. Geophys. Res. Atmos.*, **120**, 10 214–10 228, doi:[10.1002/2015JD023657](https://doi.org/10.1002/2015JD023657).
- Fueglistaler, S., and P. H. Haynes, 2005: Control of interannual and longer-term variability of stratospheric water vapor. *J. Geophys. Res.*, **110**, D24108, doi:[10.1029/2005JD006019](https://doi.org/10.1029/2005JD006019).
- , and Q. Fu, 2006: Impact of clouds on radiative heating rates in the tropical lower stratosphere. *J. Geophys. Res.*, **111**, D23202, doi:[10.1029/2006JD007273](https://doi.org/10.1029/2006JD007273).
- , M. Bonazzola, P. H. Haynes, and T. Peter, 2005: Stratospheric water vapor predicted from the Lagrangian temperature history of air entering the stratosphere in the tropics. *J. Geophys. Res.*, **110**, D08107, doi:[10.1029/2004JD005516](https://doi.org/10.1029/2004JD005516).
- , A. E. Dessler, T. J. Dunkerton, I. Folkins, Q. Fu, and P. W. Mote, 2009a: Tropical tropopause layer. *Rev. Geophys.*, **47**, RG1004, doi:[10.1029/2008RG000267](https://doi.org/10.1029/2008RG000267).
- , B. Legras, A. Beljaars, J.-J. Morcrette, A. Simmons, A. M. Tompkins, and S. Uppala, 2009b: The diabatic heat budget of the upper troposphere and lower/mid stratosphere in ECMWF reanalyses. *Quart. J. Roy. Meteor. Soc.*, **135**, 21–37, doi:[10.1002/qj.361](https://doi.org/10.1002/qj.361).
- , P. H. Haynes, and P. M. Forster, 2011: The annual cycle in lower stratospheric temperatures revisited. *Atmos. Chem. Phys.*, **11**, 3701–3711, doi:[10.5194/acp-11-3701-2011](https://doi.org/10.5194/acp-11-3701-2011).
- Gebhardt, C., and Coauthors, 2014: Stratospheric ozone trends and variability as seen by SCIAMACHY during the last decade. *Atmos. Chem. Phys.*, **14**, 831–846, doi:[10.5194/acp-14-831-2014](https://doi.org/10.5194/acp-14-831-2014).
- Gottelman, A., P. M. de F. Forster, M. Fujiwara, Q. Fu, H. Vömel, L. K. Gohar, C. Johanson, and M. Ammerman, 2004: Radiation balance of the tropical tropopause layer. *J. Geophys. Res.*, **109**, D07103, doi:[10.1029/2003JD004190](https://doi.org/10.1029/2003JD004190).
- Gilford, D. M., S. Solomon, and R. W. Portmann, 2016: Radiative impacts of the 2011 abrupt drops in water vapor and ozone in the tropical tropopause layer. *J. Climate*, **29**, 595–612, doi:[10.1175/JCLI-D-15-0167.1](https://doi.org/10.1175/JCLI-D-15-0167.1).
- Grise, K. M., and D. W. J. Thompson, 2013: On the signatures of equatorial and extratropical wave forcing in tropical tropopause layer temperatures. *J. Atmos. Sci.*, **70**, 1084–1102, doi:[10.1175/JAS-D-12-0163.1](https://doi.org/10.1175/JAS-D-12-0163.1).
- , —, and P. M. Forster, 2009: On the role of radiative processes in stratosphere–troposphere coupling. *J. Climate*, **22**, 4154–4161, doi:[10.1175/2009JCLI2756.1](https://doi.org/10.1175/2009JCLI2756.1).
- Hartmann, D. L., J. R. Holton, and Q. Fu, 2001: The heat balance of the tropical tropopause, cirrus, and stratospheric dehydration. *Geophys. Res. Lett.*, **28**, 1969–1972, doi:[10.1029/2000GL012833](https://doi.org/10.1029/2000GL012833).
- Hegglin, M. I., and Coauthors, 2013: SPARC data initiative: Comparison of water vapor climatologies from international satellite limb sounders. *J. Geophys. Res. Atmos.*, **118**, 11 824–11 846, doi:[10.1002/jgrd.50752](https://doi.org/10.1002/jgrd.50752).
- Hirota, I., 1980: Observational evidence of the semiannual oscillation in the tropical middle atmosphere—A review. *Pure Appl. Geophys.*, **118**, 217–238, doi:[10.1007/BF01586452](https://doi.org/10.1007/BF01586452).
- Kim, J., and S.-W. Son, 2012: Tropical cold-point tropopause: Climatology, seasonal cycle, and intraseasonal variability derived

- from COSMIC GPS radio occultation measurements. *J. Climate*, **25**, 5343–5360, doi:[10.1175/JCLI-D-11-00554.1](https://doi.org/10.1175/JCLI-D-11-00554.1).
- Konopka, P., J.-U. Groöf, G. Günther, F. Ploeger, R. Pommrich, R. Müller, and N. Livesey, 2010: Annual cycle of ozone at and above the tropical tropopause: Observations versus simulations with the Chemical Lagrangian Model of the Stratosphere (CLaMS). *Atmos. Chem. Phys.*, **10**, 121–132, doi:[10.5194/acp-10-121-2010](https://doi.org/10.5194/acp-10-121-2010).
- Liu, C., E. Zipser, T. Garrett, J. H. Jiang, and H. Su, 2007: How do the water vapor and carbon monoxide “tape recorders” start near the tropical tropopause? *Geophys. Res. Lett.*, **34**, L09804, doi:[10.1029/2006GL029234](https://doi.org/10.1029/2006GL029234).
- Livesey, N. J., and Coauthors, 2011: Version 3.3 level 2 data quality and description document. JPL Doc. D-33509, Jet Propulsion Laboratory, Pasadena, CA, 156 pp. [Available online at http://mhs.jpl.nasa.gov/data/v3-3_data_quality_document.pdf.]
- Maeda, K., 1987: Annual and semiannual oscillations of stratospheric ozone. *Pure Appl. Geophys.*, **125**, 147–165, doi:[10.1007/BF00878619](https://doi.org/10.1007/BF00878619).
- Maycock, A. C., K. P. Shine, and M. M. Joshi, 2011: The temperature response to stratospheric water vapour changes. *Quart. J. Roy. Meteor. Soc.*, **137**, 1070–1082, doi:[10.1002/qj.822](https://doi.org/10.1002/qj.822).
- , M. M. Joshi, K. P. Shine, S. M. Davis, and K. H. Rosenlof, 2014: The potential impact of changes in lower stratospheric water vapour on stratospheric temperatures over the past 30 years. *Quart. J. Roy. Meteor. Soc.*, **140**, 2176–2185, doi:[10.1002/qj.2287](https://doi.org/10.1002/qj.2287).
- McLandress, C., and T. C. Shepherd, 2009: Simulated anthropogenic changes in the Brewer–Dobson circulation, including its extension to high latitudes. *J. Climate*, **22**, 1516–1540, doi:[10.1175/2008JCLI2679.1](https://doi.org/10.1175/2008JCLI2679.1).
- Ming, A., P. Hitchcock, and P. Haynes, 2016: The double peak in upwelling and diabatic heating in the tropical lower stratosphere. *J. Atmos. Sci.*, **73**, 1889–1901, doi:[10.1175/JAS-D-15-0293.1](https://doi.org/10.1175/JAS-D-15-0293.1).
- Mote, P. W., and Coauthors, 1996: An atmospheric tape recorder: The imprint of tropical tropopause temperatures on stratospheric water vapor. *J. Geophys. Res.*, **101**, 3989–4006, doi:[10.1029/95JD03422](https://doi.org/10.1029/95JD03422).
- , T. J. Dunkerton, M. E. McIntyre, E. A. Ray, P. H. Haynes, and J. M. Russell III, 1998: Vertical velocity, vertical diffusion, and dilution by midlatitude air in the tropical lower stratosphere. *J. Geophys. Res.*, **103**, 8651–8666, doi:[10.1029/98JD00203](https://doi.org/10.1029/98JD00203).
- NASA, 2014: EOS Microwave Limb Sounder (MLS) Level 2 version 3.3. Subset: Daily, 2005–2013, Goddard Earth Sciences Data and Information Services Center, accessed 10 November 2014. [Available online at <https://disc.sci.gsfc.nasa.gov/Aura/data-holdings/MLS>.]
- Neale, R. B., and Coauthors, 2010: Description of the NCAR Community Atmosphere Model (CAM 4.0). NCAR Tech. Note NCAR/TN-485+STR, 212 pp. [Available online at www.cesm.ucar.edu/models/ccsm4.0/cam/docs/description/cam4_desc.pdf.]
- Newman, P. A., and J. E. Rosenfield, 1997: Stratospheric thermal damping times. *Geophys. Res. Lett.*, **24**, 433–436, doi:[10.1029/96GL03720](https://doi.org/10.1029/96GL03720).
- Perliski, L. M., S. Solomon, and J. London, 1989: On the interpretation of seasonal variations of stratospheric ozone. *Planet. Space Sci.*, **37**, 1527–1538, doi:[10.1016/0032-0633\(89\)90143-8](https://doi.org/10.1016/0032-0633(89)90143-8).
- Ploeger, F., and Coauthors, 2011: Insight from ozone and water vapour on transport in the tropical tropopause layer (TTL). *Atmos. Chem. Phys.*, **11**, 407–419, doi:[10.5194/acp-11-407-2011](https://doi.org/10.5194/acp-11-407-2011).
- , and Coauthors, 2012: Horizontal transport affecting trace gas seasonality in the Tropical Tropopause Layer (TTL). *J. Geophys. Res.*, **117**, D09303, doi:[10.1029/2011JD017267](https://doi.org/10.1029/2011JD017267).
- Polvani, L. M., and S. Solomon, 2012: The signature of ozone depletion on tropical temperature trends, as revealed by their seasonal cycle in model integrations with single forcings. *J. Geophys. Res.*, **117**, D17102, doi:[10.1029/2012JD017719](https://doi.org/10.1029/2012JD017719).
- Ramanathan, V., and R. E. Dickinson, 1979: The role of stratospheric ozone in the zonal and seasonal radiative energy balance of the earth-troposphere system. *J. Atmos. Sci.*, **36**, 1084–1104, doi:[10.1175/1520-0469\(1979\)036<1084:TROSOI>2.0.CO;2](https://doi.org/10.1175/1520-0469(1979)036<1084:TROSOI>2.0.CO;2).
- Randel, W. J., 2010: Variability and trends in stratospheric temperature and water vapor. *The Stratosphere: Dynamics, Transport, and Chemistry*, L. M. Polvani, A. H. Sobel, and D. W. Waugh, Eds., Amer. Geophys. Union, doi:[10.1002/9781118666630.ch7](https://doi.org/10.1002/9781118666630.ch7).
- , and F. Wu, 2015: Variability of zonal mean tropical temperatures derived from a decade of GPS radio occultation data. *J. Atmos. Sci.*, **72**, 1261–1275, doi:[10.1175/JAS-D-14-0216.1](https://doi.org/10.1175/JAS-D-14-0216.1).
- , R. R. Garcia, and F. Wu, 2002a: Time-dependent upwelling in the tropical lower stratosphere estimated from the zonal-mean momentum budget. *J. Atmos. Sci.*, **59**, 2141–2152, doi:[10.1175/1520-0469\(2002\)059<2141:TDUITT>2.0.CO;2](https://doi.org/10.1175/1520-0469(2002)059<2141:TDUITT>2.0.CO;2).
- , F. Wu, and R. Stolarski, 2002b: Changes in column ozone correlated with the stratospheric EP flux. *J. Meteor. Soc. Japan*, **80**, 849–862, doi:[10.2151/jmsj.80.849](https://doi.org/10.2151/jmsj.80.849).
- , —, and W. R. Rios, 2003: Thermal variability of the tropical tropopause region derived from GPS/MET observations. *J. Geophys. Res.*, **108**, 4024, doi:[10.1029/2002JD002595](https://doi.org/10.1029/2002JD002595).
- , —, H. Vömel, G. E. Nedoluha, and P. Forster, 2006: Decreases in stratospheric water vapor after 2001: Links to changes in the tropical tropopause and the Brewer–Dobson circulation. *J. Geophys. Res.*, **111**, D12312, doi:[10.1029/2005JD006744](https://doi.org/10.1029/2005JD006744).
- , M. Park, F. Wu, and N. Livesey, 2007: A large annual cycle in ozone above the tropical tropopause linked to the Brewer–Dobson circulation. *J. Atmos. Sci.*, **64**, 4479–4488, doi:[10.1175/2007JAS2409.1](https://doi.org/10.1175/2007JAS2409.1).
- Reed, R. J., 1962: Some features of the annual temperature regime in the tropical stratosphere. *Mon. Wea. Rev.*, **90**, 211–215, doi:[10.1175/1520-0493\(1962\)090<0211:SFOTAT>2.0.CO;2](https://doi.org/10.1175/1520-0493(1962)090<0211:SFOTAT>2.0.CO;2).
- , and C. L. Vilek, 1969: The annual temperature variation in the lower tropical stratosphere. *J. Atmos. Sci.*, **26**, 163–167, doi:[10.1175/1520-0469\(1969\)026<0163:TATVIT>2.0.CO;2](https://doi.org/10.1175/1520-0469(1969)026<0163:TATVIT>2.0.CO;2).
- Reid, G. C., 1994: Seasonal and interannual temperature variations in the tropical stratosphere. *J. Geophys. Res.*, **99**, 18 923–18 932, doi:[10.1029/94JD01830](https://doi.org/10.1029/94JD01830).
- Rosenlof, K., 1995: Seasonal cycle of the residual mean meridional circulation in the stratosphere. *J. Geophys. Res.*, **100**, 5173–5191, doi:[10.1029/94JD03122](https://doi.org/10.1029/94JD03122).
- Schoeberl, M. R., and A. E. Dessler, 2011: Dehydration of the stratosphere. *Atmos. Chem. Phys.*, **11**, 8433–8446, doi:[10.5194/acp-11-8433-2011](https://doi.org/10.5194/acp-11-8433-2011).
- , B. N. Duncan, A. R. Douglass, J. Waters, N. Livesey, W. Read, and M. Filipiak, 2006: The carbon monoxide tape recorder. *Geophys. Res. Lett.*, **33**, L12811, doi:[10.1029/2006GL026178](https://doi.org/10.1029/2006GL026178).
- , and Coauthors, 2008: QBO and annual cycle variations in tropical lower stratosphere trace gases from HALOE and Aura MLS observations. *J. Geophys. Res.*, **113**, D05301, doi:[10.1029/2007JD008678](https://doi.org/10.1029/2007JD008678).
- Solomon, S., K. H. Rosenlof, R. W. Portmann, J. S. Daniel, S. M. Davis, T. J. Sanford, and G.-K. Plattner, 2010: Contributions of stratospheric water vapor to decadal changes in the rate of global warming. *Science*, **327**, 1219–1223, doi:[10.1126/science.1182488](https://doi.org/10.1126/science.1182488).

- Stolarski, R. S., D. W. Waugh, L. Wang, L. D. Oman, A. R. Douglass, and P. A. Newman, 2014: Seasonal variation of ozone in the tropical lower stratosphere: Southern tropics are different from northern tropics. *J. Geophys. Res. Atmos.*, **119**, 6196–6206, doi:[10.1002/2013JD021294](https://doi.org/10.1002/2013JD021294).
- Stuber, N., M. Ponater, and R. Sausen, 2001: Is the climate sensitivity of ozone perturbations enhanced by stratospheric water vapor feedback? *Geophys. Res. Lett.*, **28**, 2887–2890, doi:[10.1029/2001GL013000](https://doi.org/10.1029/2001GL013000).
- Tegtmeier, S., and Coauthors, 2013: SPARC data initiative: A comparison of ozone climatologies from international satellite limb sounders. *J. Geophys. Res. Atmos.*, **118**, 12 229–12 247, doi:[10.1002/2013JD019877](https://doi.org/10.1002/2013JD019877).
- Ueyama, R., and J. M. Wallace, 2010: To what extent does high-latitude wave forcing drive tropical upwelling in the Brewer–Dobson circulation? *J. Atmos. Sci.*, **67**, 1232–1246, doi:[10.1175/2009JAS3216.1](https://doi.org/10.1175/2009JAS3216.1).
- Wang, Y., H. Su, J. H. Jiang, N. J. Livesey, M. L. Santee, L. Froidevaux, W. G. Read, and J. Anderson, 2016: The linkage between stratospheric water vapor and surface temperature in an observation-constrained coupled general circulation model. *Climate Dyn.*, doi:[10.1007/s00382-016-3231-3](https://doi.org/10.1007/s00382-016-3231-3).
- Wright, J. S., and S. Fueglistaler, 2013: Large differences in the diabatic heat budget of the tropical UTLS in reanalyses. *Atmos. Chem. Phys.*, **13**, 9565–9576, doi:[10.5194/acp-13-9565-2013](https://doi.org/10.5194/acp-13-9565-2013).
- Yulaeva, E., J. R. Holton, and J. M. Wallace, 1994: On the cause of the annual cycle in tropical lower-stratospheric temperatures. *J. Atmos. Sci.*, **51**, 169–174, doi:[10.1175/1520-0469\(1994\)051<0169:OTCOTA>2.0.CO;2](https://doi.org/10.1175/1520-0469(1994)051<0169:OTCOTA>2.0.CO;2).